Arabian Journal of Chemistry (2015) xxx, xxx–xxx

King Saud University

Arabian Journal of Chemistry

www.ksu.edu.sa
www.sciencedirect.com

ORIGINAL ARTICLE

# Synthesis of graphene oxide–methacrylic acid–sodium allyl sulfonate copolymer and its tanning properties

**Shenghua Lv** *, **Qingfang Zhou, Yaya Cui, Wenqiang Yang, Ying Li**

*College of Resource and Environment, Shaanxi University of Science and Technology, Xi'an 710021, China*

Received 21 March 2015; accepted 2 July 2015

**KEYWORDS**

Graphene oxide;
Copolymer;
Nanoeffects;
Synergistic effects;
Shrinkage temperature

**Abstract** Graphite oxide nanosheets (GONs) and the copolymer of GONs with methacrylic acid (MAA) and sodium allyl sulfonate (SAS) (poly(GON–MAA–SAS)) were prepared. The GONs in poly(GON–MAA–SAS) are smaller and uniformly dispersed, allowing them to penetrate into collagen fibers of leather and produce better tanning effects than current nano-tanning agents. Tanning effects due to chemical bonding and nanoeffects are elucidated by measuring the shrinkage temperature ($T_s$) of wet and dry leather. The results indicate that poly(GON–MAA–SAS) could be used alone as a tanning agent to provide excellent mechanical properties, especially good elasticity and softness, although the $T_s$ is slightly lower than that of chrome-tanned leather. Poly(GON–MAA–SAS) in combination with a chrome tanning agent could allow the dosage of the latter to be halved. These results indicate the potential for new nano-tanning agents to reduce the pollution caused by tanning agents.



## 1. Introduction

Tanning agents are the most important chemicals in the leather-making process, their function being to improve the leather's mechanical properties and hydrothermal stability (Brown and Shelly, 2011). Although, in theory, there are many chemicals that can be used as tanning agents, in practice, only trivalent chromium complexes have been successfully employed. Nowadays, chrome-tanned leather has accounted for 90% of total leather production (Chattopadhyay et al., 2012). However, although chrome tanning agent is effective, it has disadvantages, namely a low reaction efficiency and a low adsorption rate on collagen fibers (Zhou et al., 2012). The chrome tanning process usually needs 24–72 h, and the adsorption rate is only about 70%, which means that 30% of the chrome tanning agent will be released into effluent, leading to serious trivalent chromium pollution (El Nemr et al., 2015; Sfaksi et al., 2014; Zouboulis et al., 2012). At present, the principal solutions to this problem involve the addition of high-exhaustion auxiliaries (Li et al., 2014; Nashy et al., 2012) or recycling of the chrome tanning effluent (El-Sabbagh and Mohamed, 2011).

* Corresponding author. Tel./fax: +86 29 86168291.
E-mail address: lvsh@sust.edu.cn (S. Lv).

Peer review under responsibility of King Saud University.

Production and hosting by Elsevier

http://dx.doi.org/10.1016/j.arabjc.2015.07.002
1878-5352 

Please cite this article in press as: Lv, S. et al., Synthesis of graphene oxide–methacrylic acid–sodium allyl sulfonate copolymer and its tanning properties. Arabian Journal of Chemistry (2015), http://dx.doi.org/10.1016/j.arabjc.2015.07.002

Meanwhile, attempts have been made to find less harmful tanning agents by modifying traditional chrome-free agents such as those based on zirconium (Sundarrajan et al., 2003), titanium (Seggiani et al., 2014), aluminum (Musa et al., 2011), iron (Karthikeyan et al., 2011), vegetable tanning agents (Blaschke, 2012), and aldehydes (Jayakumar et al., 2011) and by developing so-called green tanning agents such as those based on zinc (Cao et al., 2013), starch (Lu et al., 2011; Lv et al., 2012), humic acid (Bacardit et al., 2012), and organic phosphates (Fathima et al., 2011). However, these alternative methods have not proved sufficiently effective to solve the problem. The principal reason is that tanning reactions based mainly on esterification, etherification, and substitution reactions cannot be carried out rapidly and high effectively in aqueous tanning medium (Krishnamoorthy et al., 2012; Kumar et al., 2011). It appears from the current situation that no further improvements are possible in this direction. Therefore, it may now be time to seek new materials and methods for solving the problems of low efficiency and its related serious pollution.

With the advent of nanomaterials and their extraordinary properties exhibited in many applications, the development of nano-tanning agents was greatly anticipated. It was believed that such agents could possess the desirable properties of lower dosage, high efficiency, and exceptional tanning functions (Nayak et al., 2014). Therefore, in recent years, much research has been carried out on the development of some nano-tanning agents, such as nano-$SiO_2$ (Fan et al., 2004; Pan et al., 2008; Yan et al., 2008), carbon nanotubes (CNTs) (Sun et al., 2010), and nano-montmorillonite (MMT) (Bao and Ma, 2012; Gao et al., 2005), with the results shown in Table 1. These results indicate that the expected tanning effects were not manifested and that these nano-tanning agents are not yet suitable for independent use in tanning leather. The reason may be that these nano-tanning agents have larger nanosize (30–150 nm) resulting in the inability to penetrate into the fibers. Also, these nano-tanning agents lack reactive groups, and so are incapable of producing tanning effects based on the formation of chemical bonds. Furthermore, the nano-tanning agents are easily agglomerated together in water medium, resulting in a significant inhibition of nanoeffects. Whatever the cause, the weak tanning effects of the current nano-tanning agents seem to have led to a decline in interest in this approach.

Based on the above analysis, we believe that nanomaterials suitable for use as tanning agents should be carefully selected on the basis of its nanosize and chemical structure. The nanosize should be small enough to allow it to penetrate into the nanometer gaps (10–30 nm) in collagen fibers first; moreover, it should also contain some chemical groups that can form covalent cross-linked network in collagen fibers. The tanning effects consist of chemical bonding tanning effects and nano-tanning effect. The role of chemical bonding tanning effects is mainly to fix uniformly the nano-tanning agent in fibers to avoid them reunion.

Graphene oxide nanosheets (GONs) with both active chemical groups and smaller nanosize have brought new possibilities for developing nano-tanning agent. GONs are produced by oxidation of graphite to graphite oxide, which can then be easily exfoliated and smashed into GON (Lv et al., 2014). There are many active groups within the graphene oxide (GON) structure: hydroxyl, epoxide, carbonyl, carbonyl and carboxyl groups found on the surface and edges (Huang et al., 2011; Lv et al., 2013; Mkhoyan et al., 2009). The presence of these groups makes GONs hydrophilic, allowing them to be easily dispersed in water (Singh et al., 2011; Dreyer et al., 2010). These groups can be controlled effectively by adjusting oxidant composition and oxidization processing (Chua et al., 2012; Chee et al., 2012). Single-layer GONs can be randomly bent and wrinkled, and multilayer GON aggregates can slide over each other. This makes it easier to become inserted in the gaps between fibers. Some researchers have started using GON to modify carbon fiber for significantly improving its applied properties (Lu et al., 2014). These research results here gave us some inspiration for developing GON tanning agent. The tanning effect of GONs has been studied in previous research by us. The research results indicate that GONs are easy to disperse in aqueous; however, they also easily reunite and aggregate, thus restricting their penetration into collagen fibers. In the work described here, a copolymer of GON with methacrylic acid (MAA) and sodium allyl sulfonate (SAS) (poly(GON–MAA–SAS)) was prepared with the aim of forming a uniform and smaller nano-sized GON dispersion and investigating its tanning effects. The results will have a positive consequence for the development of new nano-tanning agents and reducing pollution from tanning agents.

**Table 1** Tanning effects of the current nano-tanning agents.

| Nanomaterial | Application and dosage (% by weight of skin) | $T_s$ (°C) | Leather mechanical properties | | | Reference |
|---|---|---|---|---|---|---|
| | | | Tensile strength ($N/mm^2$) | Tear strength (N/mm) | Elongation at break (%) | |
| $SiO_2$, D 60–150 nm | 5% Oxazolidine–$SiO_2$ | 95.3 | 21.63 | 42.56 | 41.52 | Nayak et al. (2014) |
| $SiO_2$, D 50–80 nm | 0.2% | 86.4 | 21.41 | 38.92 | 38.92 | Yan et al. (2008) |
| $SiO_2$, D 30–50 nm | 6% poly(MAA–BA)/$SiO_2$ | 74.2 | 22.65 | 43.88 | 53.8 | Fan et al. (2004) |
| $SiO_2$, D 30–50 nm | 6%Poly(M AA–BA)/$SiO_2$ + 2% Cr | 95.8 | 24.06 | 54.6 | 74.3 | Fan et al. (2004) |
| CNTs, D 0.33 nm, L 330 nm | 0.1% CNTs + 6% Cr | 106.2 | 14.2 | 43.5 | 50.6 | Pan et al. (2008) |
| MMT | Poly(DM–AM)/MMT 6% | 75.8 | 12.1 | 32.4 | 32.5 | Sun et al. (2010) |
| MMT, interlaminar spacing 1.99 nm | 20% MMT + 2% Cr | 90.1 | 19.12 | 55.91 | 88.95 | Bao and Ma (2012) |

$T_s$ = Shrinkage temperature; $D$ = Diameter; $L$ = Length; CNTs = Carbon nanotubes; Poly(MAA–BA), copolymer of methacrylic acid (MAA) and butyl acrylate (BA); Poly(DM–AM), a copolymer of diallyl dimethyl ammonium chloride (DM) and acrylamide (AM); Cr = Chrome tanning agent.

Please cite this article in press as: Lv, S. et al., Synthesis of graphene oxide–methacrylic acid–sodium allyl sulfonate copolymer and its tanning properties. Arabian Journal of Chemistry (2015), http://dx.doi.org/10.1016/j.arabjc.2015.07.002

## 2. Experimental

### 2.1. Main materials and chemicals

Goat acid skin is obtained by treating raw goat skin by soaking, removal of hair, liming, softening, and pickling, which can be directly tanned using nano-tanning agents. Chrome tanning agent is a commercial product, and its basicity is 33% and $Cr_2O_3$ content is 25%. The ART was an outstanding commercial acrylic resin tanning agent, which is used as control sample. $H_2SO_4$ (98%), $H_3PO_4$ (85%), $KMnO_4$, $NaNO_3$, $H_2O_2$ (30%), $(NH_4)_2SO_8$, $NaHSO_3$, methacrylic acid (MAA) and sodium allyl sulfonate (SAS) were chemical purity.

### 2.2. Preparation of GONs

A three-necked round-bottomed flask was placed in an ice bath (5 °C), and 2 g flaky graphite, 60 g $H_2SO_4$, 6 g $H_3PO_4$, and 2 g $NaNO_3$ were added and mixed well. Then, 8 g $KMnO_4$ was slowly added to the flask over 15 min under stirring. The mixture was maintained at 5 °C for 1 h and then at 35 °C for 12 h under ultrasonication. It was then diluted with 200 mL deionized water and heated to 90 °C, following which 30 g $H_2O_2$ was dripped into it over a period of 1 h. The final product was a bright yellow suspension of graphite oxide sheets, which was purified by centrifugal filtration and washed repeatedly with deionized water until the washing water had a pH of 7.0 and without $SO_4^{2-}$ in washing water (Yeh et al., 2015). An aqueous dispersion of 0.5% graphite oxide was obtained and treated with ultrasonication for 60 min to disperse graphene oxide sheets into smaller nano-sized sheets, i.e., GONs.

### 2.3. Preparation of poly(GON–MAA–SAS)

A solution of monomer mixture was obtained by mixing 15 g MAA and 4 g SAS in 10 g deionized water in a dropping funnel. An initiator solution (I) was obtained by dissolving 0.3 g $(NH_4)_2SO_4$ in 10 g deionized water in another dropping funnel, and a second initiator solution (II) was obtained by dissolving 0.3 g $NaHSO_3$ in 10 g deionized water in a third dropping funnel. The monomer mixture and the initiator solutions I and II were then added dropwise over a period of about 1 h to a three-necked round-bottomed flask with 30 g GON solution at 45 °C under stirring. The reaction was then allowed to proceed at 45 °C for 5 h. Finally, the temperature of the reaction mixture was reduced to 30 °C and its pH adjusted to 7.0 with $NaHCO_3$. The product was a copolymer of poly(GON–MAA–SAS). The copolymer content was about 20% and the GON content about 0.8%. The poly(MAA–SAS) was synthesized by copolymerization of MAA and SAS with the same proportions and polymerization process as used for poly(GON–MAA–SAS).

### 2.4. Tanning properties

The goat acid skin and an equal weight of water were put into a drum, and the pH was adjusted to 6.0 with equal weights of $NaHCO_3$ and NaAc. The poly(GON–MAA–SAS) was then added to the drum in a solid dosage of 4%/6%/8%/10%/12% by weight of the skin. The drum was rotated for 4 h, after which the pH was adjusted to 3.8 over a period of 4 h by gradual addition of 10% formic acid solution. The tanned leather was then removed from the drum and rested for 10 h before determination of $T_s$. It was then returned to the drum for neutralization, dyeing, and fat-liquoring, for which the conditions were as specified in reference by Lu et al. (2011). The poly(GON–MAA–SAS)-chrome combination tanning was performed by tanning the goat skin first with poly(GON–MAA–SAS) according to above method and then according to the chrome tanning process.

### 2.5. Measurement methods

#### 2.5.1. Structural characterization methods

The elemental compositions of graphite and GONs were determined with an energy-dispersive X-ray spectrometer (EDS) (EDAX, USA) and Vario EL (III) elemental combustion analysis (ECA) (Hanau, Germany). EDS was coupled with a scanning electron microscope (SEM) (S-4800, Hitachi, Japan). Fourier-transform infrared spectroscopy (FTIR) was obtained using an EQUINOX-55 FTIR spectrometer (Bruker, Germany). The elemental valence state on the surface of graphite and GONs was determined using a XSAM 800 X-ray photoelectron spectroscopy (XPS) (Kratos, UK). The $^1H$ NMR and $^{13}C$ NMR spectra were obtained using an INOVA 400 MHz spectrometer (AVANCE III, Switzerland) with DMSO as the solvent. The number-average molar mass ($M_n$), the weight-average molar mass ($M_w$), and the polydispersity index (PDI) were determined using a Waters 575-2414 GPC instrument (Massachusetts, USA). The morphology of the GONs was characterized using an atomic force microscope (AFM) (SPI 3800N/SPA400, Seiko, Japan). The average thickness and size of the solid GONs were obtained from the AFM by statistical analysis. The size distribution of the GO in aqueous and in poly(GON–MAA–SAS) was also characterized using a Zetasizer NANO-ZS90 laser particle analyzer (Malvern, UK).

#### 2.5.2. Characterization methods for tanning results

The $T_s$ of wet leather was tested using a MSW-YD4 shrinkage-temperature tester (Xi'an, China) in glycerol medium according to QB/T2713-2005. The $T_s$ of dry leather was measured using a differential scanning calorimeter (DSC) (200PC, Netzsch, Germany) at heating rate of 2 °C/min. The mechanical properties such as tensile strength, elongation at breakage, and tearing strength were determined using a electron tension instrument (TS2000-S, China) according to GB/T17928-1999. The water vapor permeability rates were measured according to GB/T3812-1999 using a water vapor penetration rate tester (Permatran-W3/61, Mocon, USA). The micromorphology of leather fibers was recorded using a scanning electron microscopy (SEM) (S-4800, Hitachi, Japan). The adsorption rate of the GONs was measured by a gravimetric method, which included drying, washing, and constant-weight processes. Each sample was tested three times and the average was taken.

## 3. Results and discussion

### 3.1. Structural characterization of GONs and poly(GON–MAA–SAS)

#### 3.1.1. Chemical structure characterization

Table 2 shows the chemical compositions of graphite and GONs. The results indicate that the oxygen content of

**Table 2** Chemical compositions of graphite and GONs.

| | Element content (%) | | | |
|---|---|---|---|---|
| | C | O | S | Other element |
| Graphite (EDS) | 93.53 | 1.72 | 1.78 | 2.97 |
| Graphite (ECA) | 94.35 | 1.42 | 1.67 | 2.56- |
| GONs (DES) | 62.61 | 29.75 | 4.35 | 3.29 |
| GONs (ECA) | 64.90 | 27.92 | 4.12 | 3.06 |

GONs increased to 29.75% and 27.92% that correspond to EDS and ECA, respectively. The EDS is mainly used to measure the surface's element content of materials, while ECA can determine the element content of the whole materials. The difference of the two tested results is narrow, which indicated that GONs have similar oxidation. All the oxygen elements exist as oxygen-containing groups and can further be measured using a XPS and FTIR instrument.

The valence state of carbon and content of oxygen-containing groups are measured by XPS and the results are shown in Fig. 1. The results indicate that carbon bonds in graphite are C═C and C─C. The contents of C═C and C─C are 81.13% and 18.77%, respectively, by comparing the peak area of C═C and C─C, while carbon bonds in GONs are C═C, C─OH/C─O─C, C═O and COOH, and their contents are 29.15%, 23.02%, 23.35% and 25.46%, respectively. The results suggest that GONs contain more hydroxyl, epoxyl, carbonyl and carboxyl groups.

FTIR spectra of graphite, GONs and poly(GON–MAA–SAS) are shown in Fig. 2. In the spectrum of graphite, there is an obvious absorption peak due to C═C double bonds at 1610 $cm^{-1}$, indicating that there are many such bonds in graphite. The spectrum of GON shows absorption peaks due to the hydroxyl group (─OH) at 3350 $cm^{-1}$ and the carbonyl group (─C═O) at 1730 $cm^{-1}$, as well as the ether bond (─C─O─C─) at 1420, 1100 and 1050 $cm^{-1}$, suggesting that the oxygen-contained groups ─OH, ─C═O, and C─O─C are all present in GONs. The spectrum of poly(GON–MAA–SAS) indicates that there are absorption peaks due to the methyl ($-CH_3$) and methylene groups ($-CH_2-$) at 2950, 2920, 2850, and 1370 $cm^{-1}$, the carbonyl group at 1730 $cm^{-1}$, the ester bond at 1450 and 1150 $cm^{-1}$, and the ether bond at 1230 and 1080 $cm^{-1}$, indicating that the GONs have reacted with MAA and SAS, forming poly(GON–MAA–SAS).

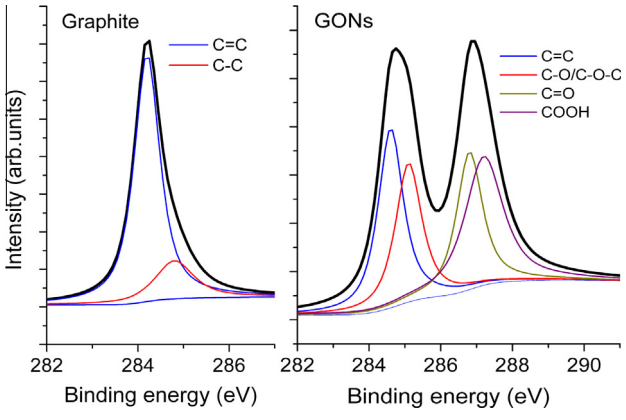


**Figure 1** XPS spectra of graphite and GONs.

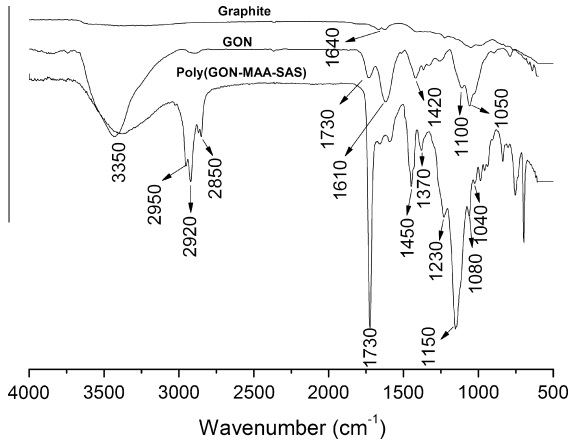


**Figure 2** FTIR spectra of graphite and GONs.

The chemical structure of poly(GON–MAA–SAS) can be determined by its NMR spectra. $^1$H NMR spectrum is shown in Fig. 3a and analyzed as follows: $^1$H NMR (400 MHz, DMSO; $\delta$, ppm): 5.71 (H12), 5.06 (H13), 4.31(H10), 3.83 (H9), 3.73 (H7), 3.46 (H8), 3.38 (H1), 2.86 (H2), 1.87 (H4), 1.45 (H3), 0.33 (H5, H11). $^{13}$C NMR spectra are shown in Fig. 3b and analyzed as follows: $^{13}$C NMR (400 MHz, DMSO; $\delta$, ppm): 178.56, 169.23, 135.46, 109.62 (characteristic peaks of C in GON), 63.62 (C5), 55.47 (C9), 53.28 (C3), 48.17 (C7), 43.84 (C2), 41.08 (C11), 35.61 (C8), 33.62 (C4), 30.6 (C1), 25.43 (C10), 13.28 (C6). The theoretical $^1$H NMR and $^{13}$C NMR data based on the given chemical structure consist with the experimental data, which proves that this chemical structure of poly(GON–MAA–SAS) has been successfully prepared.

The molecular weights and PDI of poly(GON–MAA–SAS) are shown in Table 3. The results show that their $M_w$, $M_n$ and PDI are similar, indicating that their average molecular chain lengths are similar. The molecular weight and PDI of acrylic resin tanning agents have impact on tanning effect, so the similar results could help reduce experimental error.

### 3.1.2. Size distribution of GONs

The degree of dispersion of GONs may be determined by measuring the size and thickness of GONs from its AFM morphology, which are shown in Fig. 4. About 100–150 GONs sheets

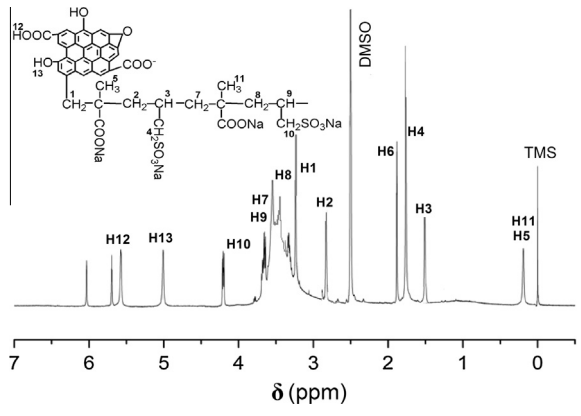


**Figure 3a** $^1$H NMR spectrum of poly(GON–MAA–SAS).

Please cite this article in press as: Lv, S. et al., Synthesis of graphene oxide–methacrylic acid–sodium allyl sulfonate copolymer and its tanning properties. Arabian Journal of Chemistry (2015), http://dx.doi.org/10.1016/j.arabjc.2015.07.002

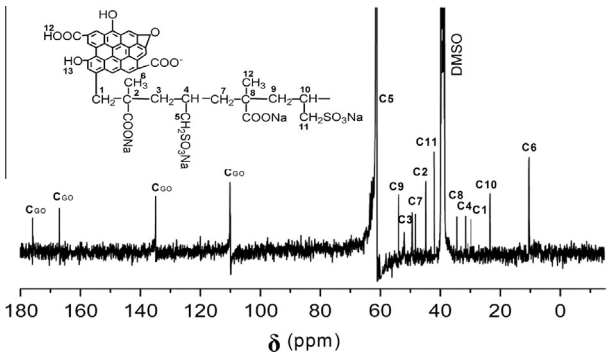


**Figure 3b** $^{13}C$ NMR spectrum of poly(GON–MAA–SAS).

**Table 3** Molecular weights and PDI of polymer tanning agents.

| Tanning agents | $M_w$ (Da) | $M_n$ (Da) | PDI ($M_w/M_n$) |
|---|---|---|---|
| Poly(GON–MAA–SAS) | 29 568 | 25 337 | 1.167 |
| Poly(MAA–SAS) | 30 631 | 26 452 | 1.158 |
| ART | 31 234 | 26 537 | 1.177 |

were statistically analyzed and the results are shown in Figs. 5a and 5b. For GONs from an aqueous medium, the average length and thickness are 100–450 and 10–17 nm, respectively. However, for GONs in poly(GON–MAA–SAS), the corresponding values are 5–60 and 1–8 nm, respectively. The results show that the average size of GONs from poly(GON–MAA–SAS) is clearly smaller than that from an aqueous. Meanwhile, Fig. 5c shows the size distribution of GONs obtained by laser particle analyzer. The results show that the size of GONs in the polymer and in an aqueous is in the ranges 1–60 nm and 50–450 nm, respectively. These results also indicate that the GONs size in the polymer is obviously smaller than that in an aqueous, and the size distribution is consistent with that by AFM. These results indicate that the GONs in poly(GON–MAA–SAS) have smaller nanosize and uniform distribution compared with those in aqueous. The smaller nanosize and uniform dispersion have a beneficial effect in improving the penetration and dispersion of GONs in collagen fibers.

### 3.1.3. Formation mechanism of poly(GON–MAA–SAS)

Based on these results above, a possible formation mechanism of GONs and poly(GON–MAA–SAS) is proposed as in Fig. 6. When the oxidants react with graphite, the oxygen-containing groups such as hydroxyl, epoxide, carbonyl and carboxyl groups, were first produced on graphite surfaces especially in its edges (Fig. 6a). With the increase of these groups, the interlaminar spacing of the edges will increase. As a consequence, the oxidants can easily penetrate deep into graphite sheets resulting in edge dilation (Fig. 6b) and reducing the molecular force. The enlarged edges will easily be exfoliated and smashed under ultrasonication (Fig. 6c). Meanwhile, the hydrophilicity of graphite oxide will obviously increase resulting in easy dispersing in aqueous. But the GONs are easily agglomerate in aqueous because of its greater surface area and high surface energy as well as self-assembled (Lu et al., 2014). Copolymerization of GON with MAA and SAS can introduce the GONs uniformly into the polymer chains through forming covalent bonding, which will achieve uniform dispersion GONs in collagen fibers (Fig. 6d).

### 3.2. Tanning effects of GONs

The tanning effects of GONs are shown in Table 4. The $T_s$ of leather tanned with GONs increased with increasing GON dosage up to 0.4% GON, with the maximum $T_s$ being 78.3 °C and 91.5 °C in the wet and dry states, respectively, while the maximum $T_s$ of leather tanned with poly(MAA–SAS) and ART was 65.6 °C and 70.4 °C, respectively, in the wet state and 66.3 °C and 71.5 °C, respectively, in the dry state. The results indicate that the $T_s$ of GON-tanned leather in both the wet and dry states is higher than that of leather tanned with any other nano-tanning agent. The $T_s$ of GON-tanned leather in the wet state reveals the tanning effects of chemical reactions, with the formation of major covalent bonds between GONs and collagen fibers that are not affected by the presence

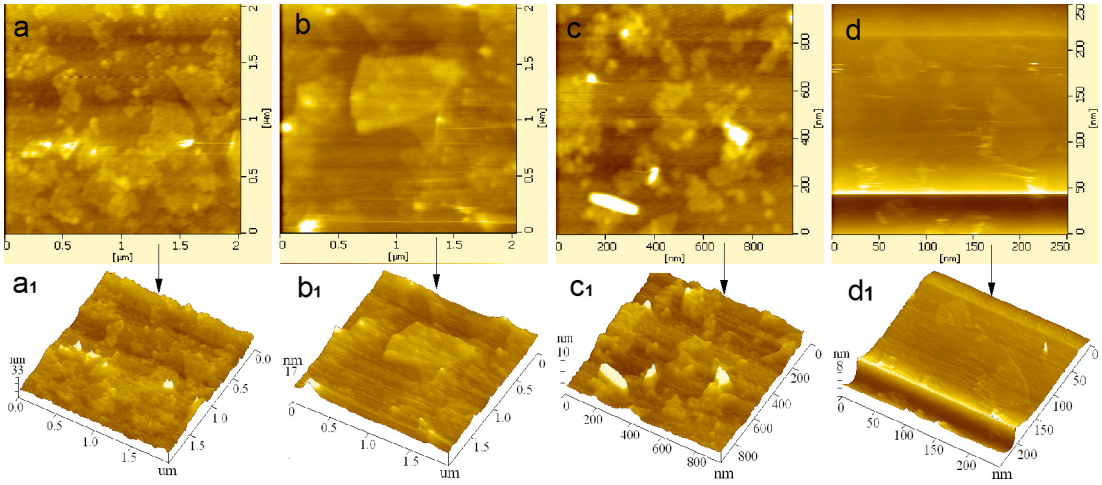


**Figure 4** AFM morphology of GONs: (a and $a_1$) from aqueous and diluted 800 times. (b and $b_1$) from aqueous and diluted 1200 times. (c and $c_1$) from poly(GON–MAA–SAS) and diluted 800 times. (d and $d_1$) poly(GON–MAA–SAS) and diluted 1200 times.

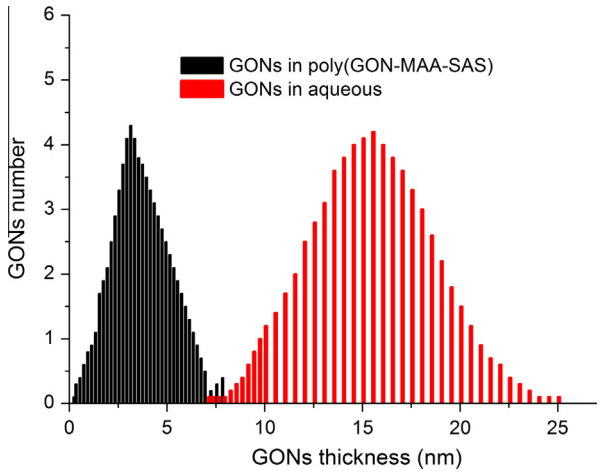


**Figure 5a** Thickness distribution of GONs by AFM.

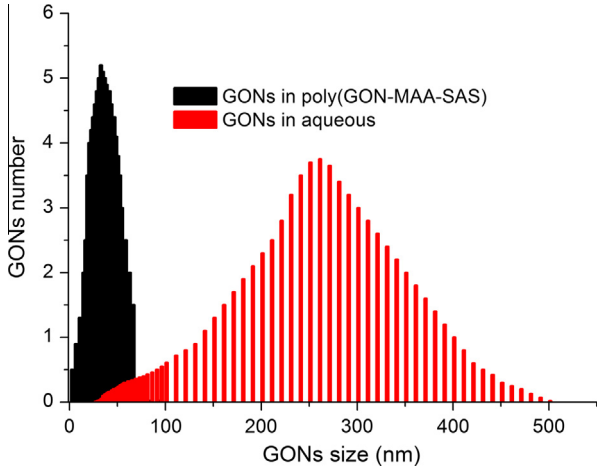


**Figure 5b** Length distribution of GONs by AFM.

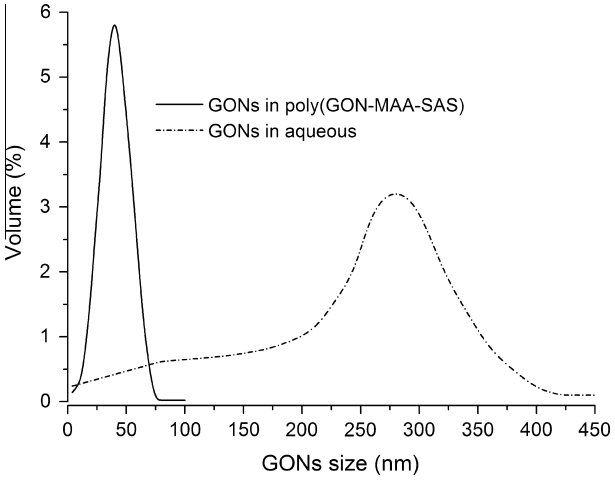


**Figure 5c** Size distribution of GONs by laser particle analyzer.

of the aqueous medium. The higher $T_s$ of dry leather reveals the contribution to tanning of nanoeffects on collagen fibers, which would be inhibited in an aqueous medium. Thus, the GON-tanned results suggest that GONs have not only a stronger chemical tanning effect than poly(MAA–SAS) but also a stronger nano-tanning effect than current nano-tanning agents. The chemical tanning and nano-tanning can together produce a synergistic effect, resulting in a more effective overall result. Furthermore, the $T_s$ of leather tanned with a chrome-tanning agent and with an acrylic resin tanning agent in both wet and dry states is very close, indicating that tanning effects are mainly based on the chemical bonds, which are less affected by the presence of an aqueous medium compared with nano-tanning effects.

As can be seen from these results, the tensile and burst strengths of GON-tanned leather are less than those of chrome-tanned leather, but the elongation at break is greater, which indicates that GONs have good lubricity properties for collagen fibers. The results also show that GON-tanned leather is soft and resilient. Thus, GON tanning effects are clearly better than those of nano-$SiO_2$, CNTs, and nano-MTT as well as those of acrylic resin tanning agents. The water vapor permeability of GON-tanned leather is increased compared with that of leather tanned with poly(MAA–SAS) or ART. This should be attributed mainly to the exceptional adsorption abilities of GON for water vapor.

For the adsorption rate of GONs in the collagen fibers, although it is higher than the adsorption rates of the current tanning agents, indicating that GON cannot totally penetrate into the collagen fibers, even though the GONs have small nanosize, the reason may be that GONs are easily agglomerated in aqueous medium, making entry into the collagen fibers difficult.

### *3.3. Tanning effects of poly(GON–MAA–SAS)*

The tanning effects of poly(GON–MAA–SAS) are shown in Table 5 and Fig. 7a. The $T_s$ of leather tanned with poly(GON–MAA–SAS) in both the wet and dry states is obviously increased, as can be seen in Fig. 7a. When leather was tanned with 10% solid dosage of poly(GON–MAA–SAS) by weight of leather, its $T_s$ reached 89.6 °C and 104.3 °C in the wet and dry states, respectively, for a GON content of only 0.4% by weight of leather. These results indicate that the $T_s$ is clearly higher than that of leather tanned using GONs or a mixture of poly(MAA–SAS) and GONs at the same dosage. The mechanical properties of leather tanned using poly(GON–MAA–SAS) are also obviously superior to those of leather tanned using GONs or a mixture of GONs and poly(MAA–SAS). The adsorption rate of poly(GON–MAA–SAS) in collagen fibers is also higher than that of GONs. These results imply that GONs in poly(GON–MAA–SAS) have smaller nanosize and uniform dispersion resulting in favoring their penetration into collagen fibers and production of both stronger chemical tanning and nano-tanning effects.

### *3.4. Tanning effects of poly(GON–MAA–SAS)-chrome combination tanning agent*

Although poly(GON–MAA–SAS) can produce good tanning effects, its performance in terms of $T_s$ and mechanical properties is slightly inferior to that of chrome tanning agents. In order to improve both $T_s$ and mechanical properties, the combined tanning effects of poly(GON–MAA–SAS) and chrome

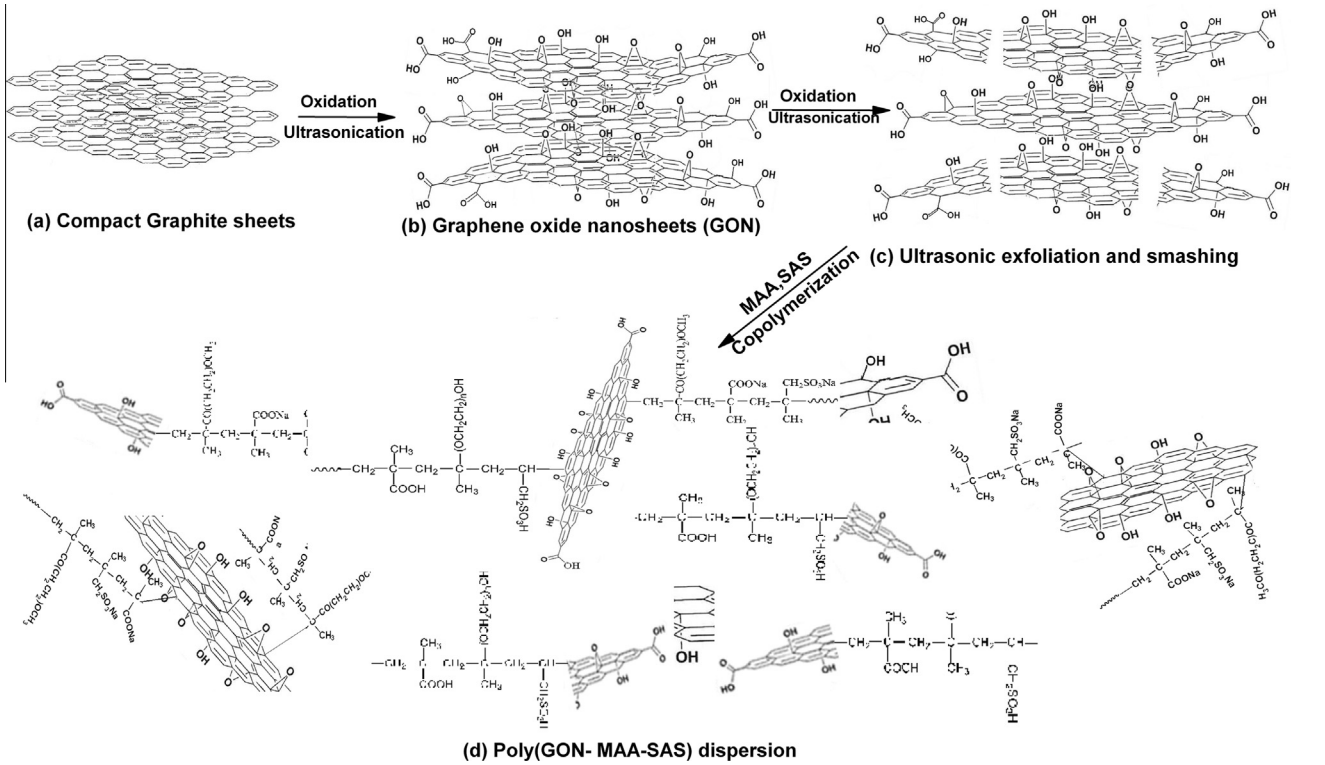


**Figure 6** The formation mechanism of GONs and poly(GON–MAA–SAS).

**Table 4** Tanning properties of GONs compared with those of other agents.

| Tanning agent dosage (%) | $T_s$ (°C) | | Mechanical properties | | | Water vapor permeability (ml/(cm$^2$ h)) | Adsorption rate (%) |
|---|---|---|---|---|---|---|---|
| | Wet leather | Dry leather | Tensile strength (MPa) | Tear strength (N/mm) | Elongation at break (%) | | |
| GON(0.16) | 65.3 | 78.3 | 14.5 | 35.4 | 41.8 | 1.78 | 70.4 |
| GON(0.24) | 73.5 | 88.3 | 16.7 | 36.7 | 55.8 | 1.82 | 67.6 |
| GON(0.32) | 76.5 | 89.6 | 19.5 | 37.5 | 63.4 | 1.94 | 65.4 |
| GON(0.40) | 78.3 | 91.5 | 21.6 | 42.5 | 63.5 | 1.98 | 65.5 |
| GON(0.48) | 78.5 | 90.5 | 22.6 | 44.1 | 63.3 | 1.86 | 63.7 |
| PMS(10.00) | 65.6 | 70.4 | 16.1 | 36.8 | 38.9 | 1.60 | 86.2 |
| ART(9.00) | 66.3 | 71.5 | 16.2 | 36.6 | 38.5 | 1.61 | 56.5 |
| Nano-$SiO_2$(0.40) | 51.2 | 53.5 | 13.2 | 28.4 | 28.6 | 1.24 | 42.5 |
| CNTs(0.40) | 52.6 | 54.3 | 14.1 | 31.1 | 31.2 | 1.37 | 41.3 |
| Nano-MMT(0.40) | 47.7 | 51.8 | 12.1 | 23.4 | 25.5 | 1.15 | 32.5 |
| Cr(8.00) | 112.5 | 113.6 | 26.5 | 61.6 | 43.7 | 1.73 | 73.6 |

PMS = Poly(MAA–SAS). Cr = Chrome tanning agent.

**Table 5** Tanning properties of poly(GON–MAA–SAS).

| PGMS (%) (GON%) | $T_s$ (°C) | | Mechanical properties | | | Water vapor permeability (ml/cm$^2$ h) | Absorption rate of GONs (%) |
|---|---|---|---|---|---|---|---|
| | Wet leather | Dry leather | Tensile strength (MPa) | Tear strength (N/mm) | Elongation at break (%) | | |
| 4(0.16) | 78.6 | 83.5 | 17.7 | 34.7 | 45.3 | 1.82 | 98.3 |
| 6(0.24) | 82.3 | 91.9 | 19.6 | 41.6 | 56.4 | 1.86 | 97.5 |
| 8(0.32) | 86.4 | 98.7 | 21.8 | 44.8 | 65.6 | 1.89 | 96.1 |
| 10(0.40) | 89.6 | 104.3 | 22.7 | 46.3 | 73.5 | 1.88 | 93.3 |
| 12(0.48) | 87.8 | 101.7 | 22.8 | 47.6 | 73.6 | 1.85 | 91.2 |
| PMS(10.00) + GON(0.40) | 77.8 | 88,5 | 18.7 | 37.6 | 55.3 | 1.84 | 75.3 |

PGMS = Poly(GON–MAA–SAS). PMS = Poly(MAA–SAS).

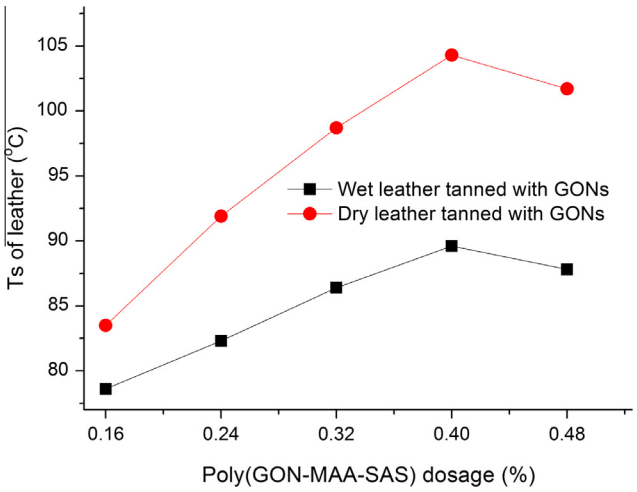


**Figure 7a** $T_s$ of leather tanned with poly(GON–MAA–SAS).

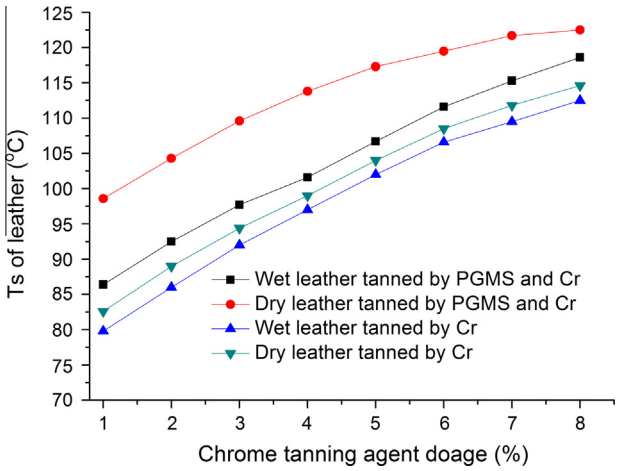


**Figure 7b** Ts of leather tanned using poly(GON–MAA–SAS)-chrome combination tanning agent (PGMS = Poly(GON–MAA–SAS, Cr = Chrome tanning agent).

tanning agents were investigated. The tanning results are shown in Table 6 and Fig. 7b, indicating that the combined tanning effects in terms of $T_s$ and mechanical properties are clearly stronger than those of poly(GON–MAA–SAS) alone or chrome tanning agent alone at the same dosage and those of the current nano-tanning agents (Table 1). For the combination tanning agent consisted by 10% poly(GON–MAA–SAS) and 3% chrome tanning agent, the $T_s$ and mechanical properties are very close to those obtained with 8% chrome tanning agent. The results show that the dosage of chrome tanning agent can be reduced by at least half in combination tanning. Meanwhile, the adsorption rate of chrome tanning agent is clearly higher than when it is used alone. The water vapor permeability of the combination-tanned leather is higher than that of leather tanned with chrome tanning agent alone. These results hint that combination tanning effects can be attributed to both chemical tanning and nanoeffects, as well as to synergistic effects. Thus, the combination tanning method could not only significantly improve their tanning effects, but also significantly reduce the dosage of chrome tanning agent required.

### *3.5. SEM images of leather tanned with poly(GON–MAA–SAS)*

SEM images of leather tanned with GONs and poly(GON–MAA–SAS) as well as with poly(GON–MAA–SAS)-chrome combination tanning agents are shown in Fig. 8. The results shown in Fig. 8(a and $a_1$) indicate that collagen fibers tanned with GONs are thicker and poorly dispersed. The reason may be that GONs easily reunite in aqueous medium, making it difficult for them to penetrate into the collagen fibers to produce tanning effects. The collagen fibers of leather tanned with poly(GON–MAA–SAS) exhibit good dispersivity compared with those tanned with GONs, as can be seen in Fig. 8(b and $b_1$). The results indicate that poly(GON–MAA–SAS) penetrates easily into the fibers to produce strong tanning effects. The reason for this may be that the poly(GON–MAA–SAS) has good dispersion and penetrating ability in collagen fibers resulting in dispersing uniformly GONs in the collagen fibers. The SEM images in Fig. 8(c and $c_1$) indicate that collagen

**Table 6** Tanning effects of poly(GON–MAA–SAS)-chrome combination tanning agent.

| Tanning agent (%) | $T_s$ (°C) | | Mechanical properties | | | Water vapor permeability (ml/cm$^2$ h) | Absorption rate of $Cr_2O_3$ (%) |
|---|---|---|---|---|---|---|---|
| | Wet leather | Dry | Tensile strength (MPa) | Tear strength (N/mm) | Elongation at break (%) | | |
| PGMS(10) + Cr(1) | 86.4 | 98.6 | 21.6 | 55.2 | 55.5 | 1.88 | 98.3 |
| PGMS(10) + Cr(2) | 92.5 | 104.3 | 24.8 | 58.3 | 65.3 | 1.93 | 97.5 |
| PGMS(10) + Cr(3) | 97.7 | 113.6 | 26.2 | 61.6 | 68.7 | 1.98 | 96.2 |
| PGMS(10) + Cr(4) | 101.6 | 115.8 | 27.5 | 62.6 | 72.2 | 1.95 | 94.3 |
| PGMS (10) + Cr(5) | 106.7 | 117.3 | 28.2 | 63.6 | 75.7 | 1.88 | 91.6 |
| PGMS (10) + Cr(6) | 111.6 | 119.5 | 28.3 | 64.8 | 74.3 | 1.87 | 89.2 |
| PGMS(10) + Cr(7) | 115.3 | 121.7 | 28.4 | 65.3 | 73.6 | 1.86 | 88.7 |
| PGMS(10) + Cr(8) | 118.6 | 122.5 | 28.6 | 66.5 | 72.4 | 1.85 | 86.3 |
| Cr(1) | 79.8 | 80.6 | 15.4 | 39.4 | 46.8 | 1.68 | 94.6 |
| Cr(3) | 92.5 | 93.4 | 16.5 | 49.4 | 56.8 | 1.71 | 88.2 |
| Cr(6) | 106.6 | 107.5 | 25.5 | 57.4 | 58.2 | 1.72 | 78.6 |
| Cr(8) | 112.5 | 113.6 | 26.5 | 61.6 | 43.7 | 1.73 | 73.6 |

PGMS = poly(GON–MAA–SAS); Cr = Chrome tanning agent.

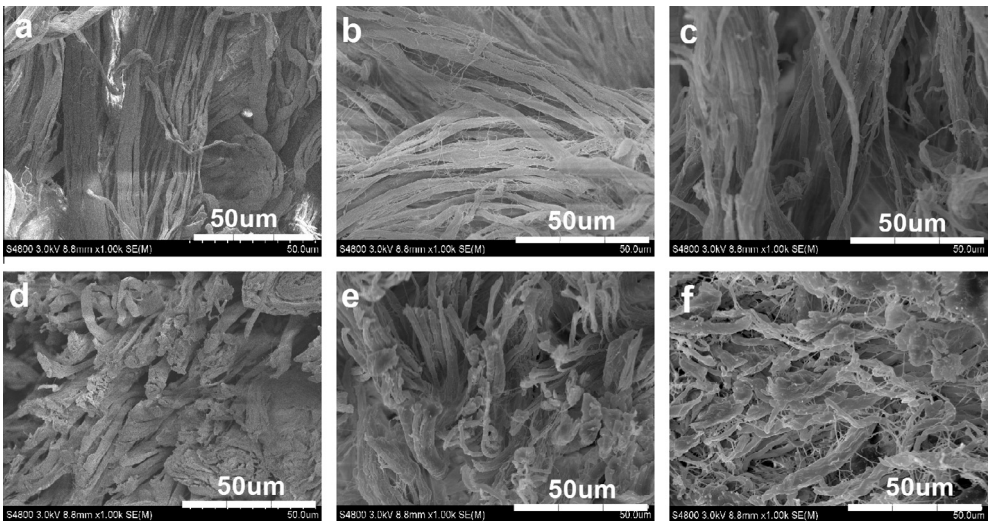


**Figure 8** SEM images of leather tanned with different tanning agents. (a and $a_1$) 0.04% GON. (b and $b_1$) 10% poly(GON–MAA–SAS). (c and $c_1$) 10% poly(GON–MAA–SAS) and 3% chrome tanning agent. (a, b and c) SEM images of longitudinal sections. ($a_1$, $b_1$ and $c_1$) SEM images of cross sections.

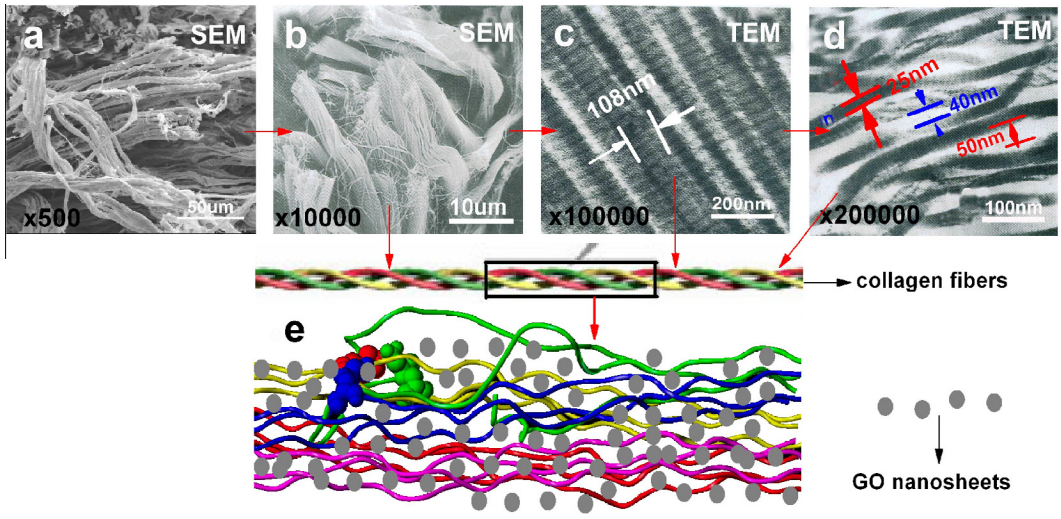


**Figure 9** (a, b, c and d) Micromorphology of collagen fibers at high magnification. (e) Schematic diagram of tanning mechanism of poly(GON–MAA–SAS).

fibers tanned with poly(GON–MAA–SAS)-chrome combination tanning agent also exhibit good dispersion. This may be because both components of the combination have excellent penetrating and dispersive as well as tanning effects. In summary, the SEM micromorphology indicates that the collagen fibers tanned with poly(GON–MAA–SAS) have better dispersion.

### *3.6. Tanning mechanism of poly(GON–MAA–SAS)*

The tanning mechanism of poly(GON–MAA–SAS) is shown in Fig. 9. Fig. 9a–d shows the micromorphology of the collagen fibers before tanning at different magnification. Fig. 9a is a SEM image of the collagen fibers at 500 times magnification, indicating that goat skin consists of many thick, spirally fiber bundles. When a thick fiber bundle in Fig. 9a is magnified to $1 \times 10^4$ times its normal size under SEM, it is found that the original apparently fiber bundle is composed of many thinner linear fibers (Fig. 9b). In fact, these thinner linear fibers themselves consist of many ultrafine collagen fibers, as can be seen in the transmission electron microscope (TEM) images in Fig. 9c and d, which are magnified to $10^5$ times normal size, respectively. The TEM images indicate that the collagen fibers are intertwined spirally, with nanometer spacing between fibers.

A schematic diagram of the tanning process is shown in Fig. 9e. A nano-tanning agent should first be able to penetrate into the nanometer spacing in the fibers, and then form chemical bonds between the fibers to produce tanning effects. The role of chemical bonding is mainly to fix and distribute uniformly GONs in fibers to avoid them reunion. Of course, GONs contained in poly(GON–MAA–SAS) are small and should easily penetrate the spaces between collagen fibers to

produce a stronger cross-linked network by both the formation of chemical bonds and nanoeffects. This speculation appears to be consistent with the results of previous studies.

## 4. Conclusions

GONs were obtained by oxidizing graphite and dispersal with ultrasonication. GONs were then copolymerized with MAA and SAS to produce poly(GON–MAA–SAS). The results demonstrated that the production of poly(GON–MAA–SAS) could allow GONs to form stable and uniform dispersions with smaller size. The tanning results indicated that the tanning effects of GONs, especially when in the form of poly(GON–MAA–SAS), were significantly better than those of other current nano-tanning agents. The reason may be that the poly(GON–MAA–SAS) can bring GONs into the collagen fibers and disperse uniformly in fibers, thereby favoring the generation of stronger tanning effects through the formation of chemical bonds and nanoeffects, as well as synergistic effects. Meanwhile, it should be possible to halve the amount of chrome tanning agent necessary to produce excellent tanning effects by using it in combination with poly(GON–MAA–SAS). Nano-tanning effects of GONs were investigated by measuring the $T_s$ of tanned leather in both wet and dry states. The $T_s$ of wet leather can be used to elucidate the contribution of chemical bonds' formation to tanning, while the $T_s$ of dry leather can be used to determine the contribution of nanoeffects. These results indicate a possible route toward making the preparation of leather a greener and cleaner process.

## Acknowledgment

We would like to thank China National Nature Science Foundation Commission for providing research project No. 21276152.

## References

Bacardit, A., Morera, J.M., Shendrik, A., Jorge, J., Ollé, L., 2012. J. Soc. Leather Technol. Chem. 96, 64.
Bao, Y., Ma, J.Z., 2012. J. Am. Leather Chem. Assoc. 107, 429.
Blaschke, Kristina, 2012. Restaurator 33, 76.
Brown, E.M., Shelly, D.C., 2011. J. Am. Leather Chem. Assoc. 106, 145.
Cao, S., Cheng, B.Z., Wang, Q.O., Liu, B.J., 2013. J. Am. Leather Chem. Assoc. 108, 428.
Chattopadhyay, B., Aich, A., Mukhopadhyay, S.K., 2012. J. Soc. Leather Technol. Chem. 96, 133.
Chee, S.Y., Poh, H.L., Chua, C.K., Sanek, F., Sofer, Z., Pumera, M., 2012. Phys. Chem. Chem. Phys. 14 (37), 12794.
Chua, C.K., Sofer, Z., Pumera, M., 2012. Chem. – Eur. J. 18 (42), 13453.
Dreyer, D.R., Park, S., Bielawskl, C.W., Ruoff, R.S., 2010. Chem. Soc. Rev. 39, 228.
El Nemr, A., El-Sikaily, A., Khaled, A., 2015. Arab. J. Chem. 8, 105.
El-Sabbagh, Salwa H., Mohamed, Ola A., 2011. J. Appl. Polym. Sci. 121, 979.
Fan, H.J., Shi, B., He, Q., Peng, B.Y., 2004. J. Soc. Leather Technol. Chem. 88, 139.
Fathima, N. Nishad, Rao, J. Raghava, Nair, Balachandran Unni, 2011. J. Am. Leather Chem. Assoc. 106, 249.
Gao, D.G., Ma, J.Z., Chu, Y., Lv, B., Dai, J.F., 2005. China Leather 34, 9.
Huang, X., Yin, Z., Wu, S., Qi, X., He, Q., Zhang, Q., Yan, Q., Boey, F., Zang, H., 2011. Small 7, 1876.
Jayakumar, G.C., Bala, L.S., Kanth, S.V., 2011. J. Am. Leather Chem. Assoc. 106, 50.
Karthikeyan, R., Ramesh, R., Venba, R., Ramamoorthy, Usha Babu, N.K., Ramasami, T., 2011. J. Soc. Leather Technol. Chem. 95, 171.
Krishnamoorthy, G., Sadulla, S., Sehgal, P.K., Mandal, Asit Baran, 2012. J. Hazard. Mater. 215–216, 173.
Kumar, M.P., Aravindhan, R., Sreeram, K.J., Rao, J.R., Nair, B.U., 2011. J. Am. Leather Chem. Assoc. 106, 113.
Li, C.Y., Chen, H.L., Liu, B.L., Wang, B., Luo, R., Shan, N., 2014. J. Appl. Polym. Sci. 131, 1089.
Lu, H.B., Liang, F., Gou, J.H., Leng, J.S., Du, S.Y., 2014a. Smart Mater. Struct. 23 (8), 1.
Lu, H.B., Yao, Y.T., Huang, W.M., Hui, D., 2014b. Compos. Part B – Eng. 67, 290.
Lu, S.H., Duan, J.P., Gong, R., Yan, X.L., 2011. J. Am. Leather Chem. Assoc. 106, 289.
Lv, S.H., Gong, R., Yan, X.L., Hou, M.M., Zhang, G.Y., 2012. J. Appl. Polym. Sci. 125, 541.
Lv, S.H., Ma, Y.J., Qiu, C.C., Sun, T., Liu, J.J., Zhou, Q.F., 2013. Constr. Build. Mater. 49, 121.
Lv, S.H., Sun, T., Liu, J.J., Zhou, Q.F., 2014. CrystEngComm 16 (36), 8508.
Mkhoyan, K.A., Contryman, A.W., Silcox, J., Stewart, D.A., Eda, G., Mattevi, C., Miller, S., Chhowalla, M., 2009. Nano Lett. 9, 1058.
Musa, A.E., Aravindhan, R., Madhan, B., Rao, J. Raghava, Chandrasekaran, B., 2011. J. Am. Leather Chem. Assoc. 106, 190.
Nashy, El-Shahat H.A., Essa, Mohamed M., Hussain, Ahmed I., 2012. J. Appl. Polym. Sci. 124, 3293.
Nayak, C., Nigam, S.D., Pandey, M., Sudarsan, V., Majumder, C., Jha, S.N., Bhatacharyya, D., Vatsa, R.K., Kshirsagar, R.J., 2014. Chem. Phys. Lett. 597, 51.
Pan, H., Qi, M., Zhang, Z.H., 2008. China Leather 37, 25.
Sundarrajan, A., Madhan, B., Rao, J. Raghava, Nair, B. Unni, 2003. J. Am. Leather Chem. Assoc. 98, 101.
Seggiani, M., Puccini, M., Vitolo, S., Chiappe, C., Pomelli, C.S., Castiello, D., 2014. Clean. Technol. Environ. Policy 16, 1795.
Singh, V., Joung, D., Zhai, L., Das, S., Khondaker, S.I., Seal, S., 2011. Prog. Mater Sci. 56, 1178.
Sfaksi, Z., Azzouz, N., Abdelwahab, A., 2014. Arab. J. Chem. 7, 37.
Sun, Y.C., Ma, J.Z., Bao, Y., Yu, Y.L., 2010. China Leather 39, 18.
Yan, L., Luo, Z.Y., Fan, H.J., Liu, Y.S., Li, H., Peng, B.Y., Shi, B., 2008. J. Soc. Leather Technol. Chem. 92, 252.
Yeh, C.N., Raidongia, K., Shao, J.J., Yang, Q.H., Huang, J.X., 2015. Nat. Chem. 7 (2), 166.
Zouboulis, A.I., Samaras, P., Krestou, A., Tzoupanos, N.D., 2012. Fresen. Environ. Bull. 2, 2406.
Zhou, J., Hu, S.X., Wang, Y.N., He, Q., Liao, X.P., Zhang, W.H., Shi, B.J., 2012. J. Soc. Leather Technol. Chem. 96, 157.

Please cite this article in press as: Lv, S. et al., Synthesis of graphene oxide–methacrylic acid–sodium allyl sulfonate copolymer and its tanning properties. Arabian Journal of Chemistry (2015), http://dx.doi.org/10.1016/j.arabjc.2015.07.002